Available online at www.sciencedirect.com
ScienceDirect
Journal of Controlled Release 119 (2007) 41–51
journal of controlled release
www.elsevier.com/locate/jconrel

Poly(vinyl alcohol)-graft-poly(lactide-co-glycolide) nanoparticles for local delivery of paclitaxel for restenosis treatment

Ulrich Westedt [a], Marc Kalinowski [b], Matthias Wittmar [a], Thomas Merdan [a], Florian Unger [a], Jutta Fuchs [a], Susann Schäller [b], Udo Bakowsky [a], Thomas Kissel [a,*]

[a] *Philipps University of Marburg, Department of Pharmaceutics and Biopharmacy, Ketzerbach 63, D-35032 Marburg, Germany*
[b] *Philipps University Hospital, Department of Diagnostic Radiology, Baldingerstrasse, 35033 Marburg, Germany*

Received 31 October 2006; accepted 17 January 2007
Available online 26 January 2007

Abstract

Catheter-based local delivery of biodegradable nanoparticles (NP) with sustained release characteristics represents a therapeutic approach to reduce restenosis. Paclitaxel-loaded NP consisting of poly(vinyl alcohol)-graft-poly(lactide-co-glycolide) (PVA-g-PLGA) with varying PLGA chain length as well as poly(lactide-co-glycolide) (PLGA), were prepared by a solvent evaporation technique. NP of <180 nm in diameter characterized by photon correlation spectroscopy (PCS), scanning electron microscopy (SEM), and atomic force microscopy (AFM) are spherical and show smooth surfaces. Yields typically range from 80 to 95% with encapsulation efficiencies between 77 and 87%. The extent of initial in vitro paclitaxel release was affected by the PVA-g-PLGA composition. Blank nanoparticles from PVA_{300}-g-PLGA(30) and PVA_{300}-g-PLGA(15) showed excellent biocompatibility in rabbit vascular smooth muscle cells (RbVSMC) at polymer concentrations of 0.37 mg/ml. Paclitaxel-loaded NP have an increased antiproliferative effect on cells in comparison to free drug. Confocal laser scanning microscopy of RbVSMC confirmed cellular uptake of nanoparticles composed of fluorescently labeled PVA_{300}-g-PLGA(15) loaded with Oregon Green labeled paclitaxel. Cells showed a clearly increased fluorescence activity with a co-localization of paclitaxel and polymer nanoparticles during incubation with particle suspension. To evaluate the antirestenotic effect in vivo, paclitaxel-loaded nanoparticles were administered locally to the wall of balloon-injured rabbit iliac arteries using a porous balloon catheter. As a result a 50% reduction in neointimal area in vessel segments treated with paclitaxel-loaded nanoparticles compared to control vessel segments could be observed (local paclitaxel nanoparticle treated segments 0.80 ± 0.19 mm^2, control segments 1.58 ± 0.6 mm^2; $p < 0.05$).

Keywords: Poly(vinyl alcohol)-graft-poly(lactide-co-glycolide); Nanoparticles; Paclitaxel; Restenosis

1. Introduction

Percutaneous transluminal angioplasty is an established method to treat peripheral arterial occlusive disease. Initially success rates up to 95% are achieved; however, these results are limited by a restenosis rate occurring in 30–50% of patients within the first 3–6 months. Restenosis is a complex process involving much redundant pathology including platelet deposition and thrombus formation, inflammation, smooth muscle cell proliferation and vascular remodeling [1–3]. Presently the cause of restenosis is not completely understood. Numerous clinical trials with systemic application of antiproliferative or antithrombotic compounds have failed to prove efficacy for the prevention of restenosis following angioplasty although animal studies initially showed promising results [1,4–6].

To prevent restenosis drugs must be delivered at high concentrations for a prolonged period of time. Catheter-based local delivery of pharmacologic agents offers a potential approach to reduce restenosis, and minimizing undesirable systemic side effects. However, recent studies demonstrated that the delivery efficiency and intramural retention of directly infused drug solutions remains rather low [7,8]. Thus, colloidal drug carriers based on biodegradable polymers have been developed to provide local drug release and sustained retention

* Corresponding author. Tel.: +49 6421 2825881; fax: +49 6421 2827016.
E-mail address: kissel@staff.uni-marburg.de (T. Kissel).

0168-3659/$ - see front matter © 2007 Elsevier B.V. All rights reserved.
doi:10.1016/j.jconrel.2007.01.009

of drug in the arterial wall. Recent studies have demonstrated that nanoparticles can be delivered more efficiently to the arterial tissue than microparticles [9–11]. Numerous drugs were investigated for the inhibition of intimal thickening [6]. A promising approach to inhibit restenosis is the controlled release of paclitaxel [12,13]. Paclitaxel, a very potent antiproliferative drug which binds to the β-subunits of tubulin, promotes the formation of extremely stable and non-functional microtubule bundles. As a result, cell replication is blocked in late G2 and M phase of the cell cycle [14]. Due to the poor solubility of paclitaxel in water, the solvent displacement technique [15], which is widely used for encapsulation of lipophilic drugs, is an attractive method to form nanoparticles. Various types of biodegradable polymers such as polylactide (PLA) [1,16], poly (lactide-co-glycolide) (PLGA) [17,18], or polycaprolactone (PCL) [19] have been used to formulate sustained release nanoparticles. In the present study, nanoparticles from biodegradable comb polyesters [20,21] were prepared using the solvent displacement method. These brush-like grafted polyesters consist of a hydrophilic polymer backbone, PVA, onto which hydrophobic PLGA is grafted. This polymer structure offers various possibilities to modify drug release kinetics. Firstly, water uptake and swelling properties of the matrix can be varied by changing the hydrophilic part of the polymer. Or secondly, degradation and release behavior can be modified by grafting PLGA with different chain length onto the backbone [22].

Our study was carried out to characterize nanoparticles from PVA-g-PLGA comb polyesters with regard to their applicability as vascular paclitaxel delivery system by investigating drug release, in vitro cytotoxicity, and cellular uptake behavior, as well as in vivo efficacy in a New Zealand white rabbit stenotic iliac artery model.

2. Materials and methods

2.1. Materials

Linear PLGA 50:50 (RG 503H, Mw 28,000 g/mol was supplied by Boehringer Ingelheim (Germany). Paclitaxel (Genexol™) was kindly provided by Sam Yang Corp. (Seoul, Korea). Radio-labeled paclitaxel (paclitaxel-[2-benzoyl ring-UL-^{14}C]) was obtained from Sigma (Sigma Chemicals, Germany). Oregon Green labeled Paclitaxel and 7-methoxy-coumarin-3-carbonyl azide for fluorescence labelling of PVA_{300}-g-PLGA was purchased from Molecular Probes (Leiden, Netherlands). Poloxamer 188 was supplied by BASF (Pluronic F 68™, BASF Parsippany, NJ). The liquid scintillation cocktail was obtained from Packard BioScience (Ultima Gold™ LS cocktail, Groningen, Netherlands). All other chemicals of analytical grade were purchased from Sigma (St. Louis, MO).

2.2. Poly((vinyl alcohol)-g-(D,L-lactide-co-glycolide))

Synthesis and characterization were described elsewhere [22]. Briefly, comb polyesters were synthesized by a stannous octoate catalyzed ring-opening polymerization of lactide and glycolide (1:1) in the presence of the backbone poly(vinyl alcohol) (PVA; Mw 15 kg/mol, polymerization degree 300, hydrolysis degree 88%) under anhydrous conditions. The polymers used for nanoparticle preparation were described in Table 1. The following nomenclature will be used to specify the polymers: PVA_{300}-g-PLGA(XX). The number in parenthesis refers to the mass ratio of branched PLGA, which is grafted (g) onto hydrophilic backbone, compared to the PVA.

For cellular nanoparticle uptake studies PVA_{300}-g-PLGA (15) was fluorescence labeled as follows: 7-methoxy-coumarin-3-carbonyl azide was added to a solution of the polymer in *N*-methyl-pyrrolidone. The reaction mixture was stirred at 80 °C for 4 h. After cooling to room temperature, the solution was poured into demineralized water and the precipitate was collected by filtration. The product was washed several times and dried in a vacuum chamber at room temperature for 6 days. The theoretical degree of substitution was 9.6%. Infrared and ^{1}H NMR spectroscopy confirmed the coupling of the fluorescent marker to the polymer with an excitation wavelength of 340 nm and an emission wavelength of 430 nm as determined by fluorescence spectroscopy.

2.3. Nanoparticle preparation

Nanoparticles were formed by a modified solvent displacement technique, described in detail elsewhere [23]. Briefly, polymer (20 mg) and paclitaxel (0, 0.5, 1, 2 mg) were co-dissolved in 2 ml acetone. The resulting solution was added at constant flow rate of 10.0 ml/min to 10 ml of a stirred (500 rpm) aqueous phase of filtrated (0.2 μm, Schleicher & Schuell, Germany) and double-distilled water containing 0.1% (m/m) poloxamer 188 (Pluronic™ F68) using a syringe with injection needle (Sterican™ 0.6×25 mm; B Braun, Melsungen, Germany). For the release study, nanoparticles were directly

Table 1
Characteristics of biodegradable polymers based on PVA-g-PLGA comb polyesters and PLGA

Number	Polymer	Polymer properties			
		Mw[a] (kg/mol)	Mn[a] (kg/mol)	Side chain length[b] (monomer units)	Ratio lactide: glycolide
1	PVA_{300}-g-PLGA(10)	156.2	116.4	12.9	1:1
2	PVA_{300}-g-PLGA(15)	249.9	178.7	17.8	1:1
3	PVA_{300}-g-PLGA(30)	438.1	319.1	31.7	1:1
4	Coumarin-PVA_{300}-g-PLGA(15)	331.1	190.6	17.8	1:1
5	Linear PLGA[c]	28.4	–	–	–

[a] Determined by SEC (size exclusion chromatography) combined with MALLS (multi angle laser light scattering) using *N,N* dimethylacetamide containing 2.5 g/l LiBr as eluent.

[b] PLGA side chain length determined from ^{1}H NMR is given as average number of monomer units on the PVA backbone (Mw_{PVA} = 15 kg/mol).

[c] RG503H, supplied by Boehringer Ingelheim, Germany.

prepared in the release medium composed of a phosphate buffered (0.05 M, I=0.01, pH 7.4) poloxamer 188 solution. The resulting colloidal suspension was stirred for 2 h under reduced pressure to remove residual organic solvent. The nanoparticle suspension was stored at 4 °C until use. For determination of drug loading efficiency and in vitro drug release, ^{14}C-labeled and unlabeled paclitaxel were mixed at mass ratio of 1/250. The nanoparticle yield was determined gravimetrically after preparation, and additionally, after the passage through a channelled balloon delivery catheter (SCIMED REMEDY™ model RC 20/2.5, lot 3377794, Boston Scientific, Natick, MA). The catheter, which was also used for the in vivo experiments, carries 18 channels with 1 group of 30-μm diameter pores per channel for infusion of drug solutions or particle suspensions [24]. All measurements were performed in triplicate.

Nanoparticles for cellular uptake studies were prepared from a mixture of fluorescence-labeled PVA_{300}-g-PLGA(15) and unlabeled PVA_{300}-g-PLGA(15) in a ratio of 2 to 8. Nanoparticles contained 0.1% (w/w) Oregon Green labeled paclitaxel. For in vivo experiments nanoparticles consisting of PVA_{300}-g-PLGA(30) were prepared under aseptic conditions (theoretical drug load of 2% paclitaxel (w/w)).

2.4. Nanoparticle characterization

2.4.1. Particle size measurement

For measurement of average size and size distribution of the nanoparticle suspensions by photon correlation spectroscopy (PCS) (Zetasizer 4/AZ 110; Malvern Instruments, UK), each sample was diluted with filtrated and distilled water to a nanoparticle concentration of 0.5 mg/ml to avoid multiscattering events. The photon correlation spectroscopy software V 1.26 was used to calculate mean diameter and width of fitted Gaussian distribution. Moreover, the NP size was determined after passage through the channelled balloon catheter. Each measurement was performed in triplicate.

2.4.2. Scanning electron microscopy (SEM)

The morphology of nanoparticles was characterized by SEM using a Hitachi S-4100 microscope (Hitachi, Germany). A drop of the nanoparticle suspension (2 mg/ml) was placed on a glass cover slide and dried under vacuum for 12 h. After that, the slides were mounted on aluminum pins using double-sided adhesive tape. Prior to microscopic examination the samples were coated with a gold layer under vacuum for 30 s (Edwards Auto 306, Edwards, Germany).

2.4.3. Atomic force microscopy (AFM)

A drop of the nanoparticle suspension was directly placed on a silicon chip. Atomic force microscopy was performed with a Digital Nanoscope IV Bioscope (Veeco Instruments, Santa Barbara, CA) as described elsewhere [25]. The vibration-damped microscope was equipped with pyramidal Si3N4 tips (NCH-W, Veeco Instruments, Santa Barbara, CA) on a cantilever with a length of 125 μm, a resonance frequency of about 220 kHz and a nominal force constant of 36 N/m. To avoid damage of the sample surface all measurements were performed in the tapping mode. The scan speed was proportional to the scan size with a scan frequency from 0.5 to 1.5 Hz. Images were obtained by displaying amplitude, height and phase signal of the cantilever in the trace direction recorded simultaneously.

2.4.4. Determination of encapsulation efficiency

After centrifugation of 1 ml of the nanoparticle suspension (10 min at 10 000 rpm) the clear supernatants were removed and the sediments were dissolved in acetone before mixing with 5 ml of scintillation cocktail. The activity of radio-labeled paclitaxel in supernatants and residues was quantified by liquid scintillation counting (LSC) (Tri-Carb 2100TR, Packard BioScience, Germany). The encapsulation efficiency was calculated by comparing the actual and theoretical loading in consideration of the ^{14}C-paclitaxel/paclitaxel ratio. Each sample was measured in quadruplicate.

2.5. In vitro release of paclitaxel

Nanoparticles for release experiments had a theoretical drug load of 2% (w/w). One milliliter of the nanoparticle suspension in 1.5 ml Eppendorf cups (Eppendorf, Germany) was placed in an incubator at 37 °C. At predetermined time intervals the buffer was withdrawn after centrifugation and replaced by fresh phosphate buffer (0.05 M, pH 7.4) containing 0.1% (w/w) poloxamer 188. The amount of drug released and the encapsulation efficiency were determined in quadruplicate as described above.

2.6. In vitro cell culture studies

2.6.1. Rabbit vascular smooth muscle cell (RbVSMC) culture

The cells were isolated from abdominal aortas of New Zealand white rabbits [26] and cultured in DMEM (Dulbecco's modified Eagle medium, Sigma-Aldrich, Germany) supplemented with 2 mM glutamine (Sigma-Aldrich, Germany) and 10% fetal calf serum (Gibco, Germany) at 37 °C, 95% rh. and 8.5% CO_2. Vascular smooth muscle origin was confirmed by immunocytochemical staining with monoclonal antibodies against smooth muscle alpha actin (Progen Ind., Australia). Assays were always performed in the exponential growth phase of the cells. Absence of mycoplasms was assured using the DAPI (4′6-diamidino-2-phenylindole) staining method (Molecular Probes, Leiden, The Netherlands).

2.6.2. In vitro cytotoxicity using MTT Assay

In vitro cytotoxicity of blank, paclitaxel-loaded nanoparticles from PVA_{300}-g-PLGA(15) and PVA_{300}-g-PLGA(30) with a theoretical drug load of 2% (w/w), and free paclitaxel were investigated using the primary RbVSMC culture. Nanoparticles were prepared under aseptic conditions. Paclitaxel was dissolved in 96% ethanol. To obtain different test concentrations, several dilutions of paclitaxel stock solution and nanoparticle suspensions were prepared with DMEM culture medium. Ethanol amounts used for dilution showed no influence on the cell

viability during the experiments. RbVSMC were seeded into 96-well microtiter plates (Nunclon™, Nunc, Germany) at a density of 5000 cells/well. After 24 h the culture medium was replaced with different dilutions of the stock solutions. After an incubation period of 24 h the culture medium was replaced with fresh, drug-, and nanoparticles-free culture medium. After an additional incubation time of 48 h the viability of the cells was evaluated by the MTT assay ($n=7$). MTT (3-(4,5-dimethylthiazol-2-yl)-2,5-diphenyl tetrazolium bromide) (Sigma-Aldrich, Germany) was dissolved in phosphate buffered saline at 5 mg/ml and 20 µl were added to each well reaching a final concentration of 0.5 mg MTT/ml. After an incubation time of 4 h unreacted dye was removed by aspiration, the purple formazan product was dissolved in 200 µl/well dimethyl sulfoxide and quantitated by a plate reader (Titertek Plus MS 212, ICN, Germany) at wavelengths of 570 and 690 nm.

Poly(ethylene imine) 750 kDa (BASF, Germany) at 1 mg/ml in DMEM was used as a positive control and poly(ethylene) 600 (Merck, Germany) at 1 mg/ml in DMEM as a negative control.

2.6.3. Cellular nanoparticle uptake: living cell confocal laser scanning microscopy (CLSM)

For living cell confocal microscopy experiments a Zeiss Axiovert 100 M microscope coupled to a Zeiss LSM 510 scan module was used. Cells (10,000 RbVSMC) were seeded 12 h before the experiment into 2 cm^2 self-made chamber dishes containing a total of 500 ml medium. Temperature was maintained at 37 °C for the duration of the experiment. A CO_2 atmosphere was not necessary, as the cell culture medium contained 25 mM HEPES (IMDM, PAA, Cölbe, Germany). Cells were incubated in fresh serum free media containing nanoparticles prepared from coumarin labelled PVA_{300}-g-PLGA(15) and Oregon Green labelled paclitaxel (0.1% w/w). An enterprise UV laser was used to excite the fluorescent label attached to the polymer at 364 nm and an argon laser was used for paclitaxel fluorescence at a wavelength of 488 nm. Images were recorded every 5 min in multi tracking mode using a longpass filter of 385 nm for UV-laser light and a longpass filter of 505 nm for argon laser light. For each time point several images were recorded in different layers and subsequently overlaid using Zeiss LSM 510 software. With respect to a clearer illustration of the co-localized green paclitaxel fluorescence and the blue fluorescence of the polymer, the colour of the fluorescence emitted from the polymer is displayed in red.

2.6.4. Animal experiments

All animal experiments were carried out according to the guidelines for the care of laboratory animals. The study protocol had been approved by the local animal care committee of the state government. Eight male New Zealand white rabbits (2.5–3 kg bodyweight) underwent balloon dilation of both common iliac arteries to induce an arterial stenosis. Prior to intervention animals were housed individually and were allowed to acclimate to their cages for two weeks starting with a 1% cholesterol diet after one week and water ad libitum.

Balloon denudation was performed under general anesthesia (ketamine, 50 mg/kg; xylacine, 5 mg/kg) administered in combination by intramuscular injection. To maintain anesthesia, additional doses of ketamine were given i.v. after cannulation of an ear vein as required. The right carotid artery was exposed and a 4 French arterial sheath (Terumo Corporation, Tokyo, Japan) was introduced. A standard 0.018 in. guide wire (Boston Scientific, Watertown, MA, USA) was advanced under fluoroscopic guidance into the common femoral artery. A calibrated intra-arterial angiography of the distal aorta and both iliac arteries was obtained. Then, a balloon catheter (2 cm in length, 3 mm in diameter, Viper, Boston Scientific, Watertown, MA, USA) was introduced into both common iliac arteries. The balloon, which had been inflated just distal to the aortic bifurcation was pulled back 1 cm three times resulting in a mechanical damage of the treated common iliac arteries. After denudation, additional angiography was carried out in order to detect dissections or signs of vessel perforation. The carotid artery was ligated after removal of the sheath. To prevent thrombus formation 100 I.U. (international units) heparin/kg bodyweight were given intravenously prior to intervention. The animals were kept on a 1% cholesterol diet and water ad libitum until the end of the study.

2.6.5. Application system for nanoparticles

The delivery device has been described in detail elsewhere [24]. Briefly, it consists of a three lumen over the wire catheter with separate ports for balloon dilation and local drug delivery.

The balloon carries 18 channels with one group of pores (30 µm) per channel, arranged in a spiral pattern along the entire balloon length. The catheter shaft is 3.4 French. For the purpose of this study we used a balloon length of 20 mm and a diameter of 2.5 mm.

2.6.6. Balloon angioplasty and local delivery of paclitaxel-loaded nanoparticles

Balloon dilation and local drug delivery were performed four weeks after stenosis induction under general anesthesia and sterile conditions. To prevent thrombus formation 100 I.U. heparin/kg bodyweight were given intravenously prior to the intervention.

The left carotid artery was exposed and a 4 French arterial sheath was introduced. A calibrated angiography was obtained to measure the degree of stenosis. The target vessel and the type of treatment applied were randomly selected from a computer generated randomization list prior to intervention. A 0.018 in. guide wire and a guiding catheter were advanced into the femoral arteries. Then a 0.014 guide wire (Guidant, Temecula, CA, USA) was exchanged. After insertion of the guide wire the channelled balloon catheter (Boston Scientific, Watertown, MA, USA) was advanced into the former angioplasty area and the balloon was inflated at a pressure of 8 atm. Angioplasty balloon inflation was controlled with a manometer (Encore, Boston Scientific, Watertown, MA, USA) to control the pressure during inflation. Simultaneously, nanoparticle administration of a total volume of 4 ml (corresponds to 160 µg Ptx) was performed at 2 atm through the second port of the channelled balloon catheter. Normal saline was administrated with identical application parameters to the contralateral artery, which served as a control.

After nanoparticle delivery the catheter was removed and a completion angiogram was performed. The sheath was removed and the carotid artery was ligated.

2.6.7. Histological preparations

Four weeks after balloon dilation and simultaneous local nanoparticle delivery a laparotomy was performed under general anesthesia. The infrarenal aorta was cannulated and a calibrated angiography of the iliac arteries was obtained. Then, the animals were sacrificed by a lethal dose of T61® (embutramide, mebezoniumjodide, tetracainhydrochloride; Hoechst, Frankfurt, Germany). The abdominal aorta and the iliac arteries were excised, perfused with normal saline and immersion fixed with 4% paraformaldehyde solution. A 1 cm long vessel segment of both common iliac arteries starting 1 cm distal to the aortic bifurcation was cut into 3 segments. The proximal and distal margins were marked with sutures and embedded in paraffin. The segments were cut and stained using routine methods.

After hematoxyline-eosin and van Gieson staining the segments were morphometrically analyzed using a semiautomatic planimetric system. The cross sections (4 μm) were projected onto a digital image analyzer (Leica Germany, Quantimed 600 software). The following borders were highlighted with a trackball: external elastic lamina (EEL), internal elastic lamina (IEL) and luminal/intimal border. The luminal area, intimal area (defined as the area under the IEL) and media area (defined as the area between EEL and IEL) were measured. Neointimal area and an intima (IEL — lumen)/media (EEL–IEL) ratio were also calculated. All segments were morphometrically analyzed and in all groups only the sections with the largest neointimal area identified by morphometry were used for data evaluation. All histomorphological measurements were performed by skilled observers blinded to the treatment groups. Three cross sections of each vessel segment were measured.

2.6.8. Statistical analysis

Results are expressed as mean±SEM (standard error of mean). Statistical data analysis was conducted using SPSS for Unix, Release 6.14. After confirmation of normal distribution using the Kolmogoroff–Smirnoff-Test comparison of the in vivo data was performed using Students' *t*-test. Additionally, in vivo data were compared by a one-way analysis of variance (ANOVA) followed by Fisher's *t*-test for further evaluation of the difference of two means. Predictive value (p) less than 0.05 was considered statistically significant.

3. Results and discussion

3.1. NP characterization

The solvent evaporation method appears to be particularly suitable for the preparation of PVA-g-PLGA nanoparticles [23]. The mechanism of particle formation thought to occur according to "diffusion-stranding" process found in spontaneous emulsification also designated as Marangoni-effect [27]. The morphology of nanoparticles prepared by the solvent displacement technique is exemplarily shown for NP from PVA_{300}-g-PLGA in Figs. 1 and 2. The surface of spherical NP appeared to be smooth and without pores, similar to NP from PLA, or PLGA [18,28]. The mean particle size ranged between 140 and 170 nm as confirmed by SEM (Fig. 3A). Apparently, the encapsulation of paclitaxel did not affect the nanoparticle size, or polydispersity indices (0.1 to 0.17) suggesting uniform, and monomodal size distributions. Particle yields were in the range of 80 to 94% (Fig. 3B) and comparable to recently published results [29]. The passage of nanoparticles through the channelled balloon catheter did not influence the particle size or yield, as shown in Fig. 3A and B. The encapsulation efficiency (EE) at a theoretical loading of 2% ranged from 77% for PVA_{300}-g-PLGA (10) NP to 87% for PVA_{300}-g-PLGA(30) NP. In comparison PLGA NP showed an EE of 80% equal to NP from PVA_{300}-g-PLGA(15). Based on recent published data [30,31], we can assume that at a drug load of 2% (w/w) the polymeric matrix does not contain any crystalline paclitaxel. Polymer and drug may form a molecular dispersion, in which paclitaxel was present in an amorphous or disordered crystalline phase.

In contrast to other researchers, who visualized cellular NP uptake with red fluorescence loaded nanoparticles [32,33], we prepared NP from labelled polymer using 7-methoxy-coumarin-3-aminocarbonyl-conjugated PVA_{300}-g-PLGA(15). The use of fluorescence labelled instead of fluorescence loaded particles avoids any unintentional dye release that would prevent the exact determination of the particle distribution by confocal laser scanning microscopy (CLSM). Fluorescence-labelled paclitaxel nanoparticles thus obtained for cellular uptake studies had a particle size of 118.4 nm±7.3 nm with a polydispersity index of 0.1±0.024, and additionally, show the same shape and surface characteristics as unlabelled nanoparticles (Fig. 2B).

3.2. In vitro drug release

The drug release from a nanoparticulate matrix system, in which the drug is uniformly embedded, generally occurs by diffusion or erosion of the matrix. Several parameters can affect the drug release rate from matrix systems [19]. In addition to the particle size [34] molecular weight and lactide to glycolide ratio of the polymer used as matrix forming system have an important impact on the drug release [35]. The influence of the composition of branched polyesters on the cumulative drug release of paclitaxel-loaded NP is shown in Fig. 4. An initial drug burst dominates the early release phase. In the case of PVA_{300}-g-PLGA(10) nearly 80% of the encapsulated paclitaxel was released during the first day. An increased chain length resulted in a substantial decrease of burst rates as observed for PVA_{300}-g-PLGA(15) (56%) and PVA_{300}-g-PLGA(30) NP (38%). PLGA NP exhibited the lowest burst release of ca. 35%. The following release phase of all NP species was characterized by a slow but continuous profile over a time period of 22 days. Other authors observed comparable release behavior with regard to PLGA NP [28,29]. The paclitaxel release exhibited a biphasic release pattern, which was characterized by an initial drug burst during the first 24 h, followed by a slower release phase.

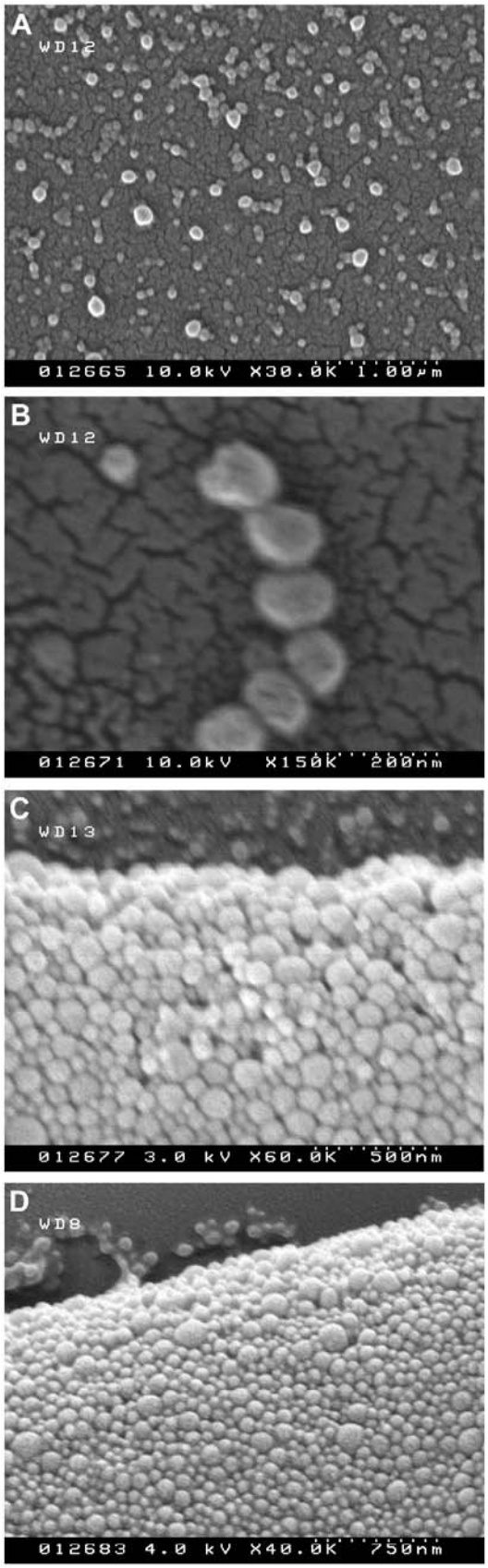

Fig. 1. Scanning electron micrographs of nanoparticles prepared from (A), (B) PVA_{300}-g-PLGA(30), (C) PVA_{300}-g-PLGA(15), and (D) fluorescence-labelled PVA_{300}-g-PLGA(15) loaded with 0.5% paclitaxel in different magnifications.

The burst release of hydrophobic paclitaxel from the nanoparticles is possibly due to the influence of the hydrophilic backbone and the PLGA chain length of the polymers. The lower the PLGA chain length the lower the lipophilicity of the polymer and the lower the solubility of paclitaxel in the polymer [31], resulting in an increased amount of free paclitaxel and a decreased EE compared to the other comb polyesters, and especially to PLGA [21].

Another important aspect is the presence of surfactant acting as stabilizing agent for the NP suspension. While the hydrophobic drug containing organic solution was added to the poloxamer 188 containing water phase, the paclitaxel might accumulate in the hydrophobic domains of the surfactant molecules. When the NP solidifies in the aqueous phase and surfactant molecules attach to the hydrophobic NP surface, the drug is not able to diffuse back into the solid core of the nanoparticles [36]. Dissolution and diffusion procedures of the drug, which was adsorbed onto the NP surface, could lead to an initial drug burst, while the slower and continuous release phase may be attributed to the diffusion of the drug localized in the NP core [37]. On the other hand, the addition of poloxamer 188 to the aqueous medium after phase mixing potentially reduces the drug release rate due to the absence of deep-seated surfactant molecules at the nanoparticle surface, as described for a lipophilic low molecular weight tyrphostin compound [34]. Ultimately, the reduction of the aqueous to organic phase ratio during nanoparticle preparation may lead to initial higher drug release rates [38]. Accordingly, drug escapes from pre-formed nanoparticles due to the external medium rich of organic

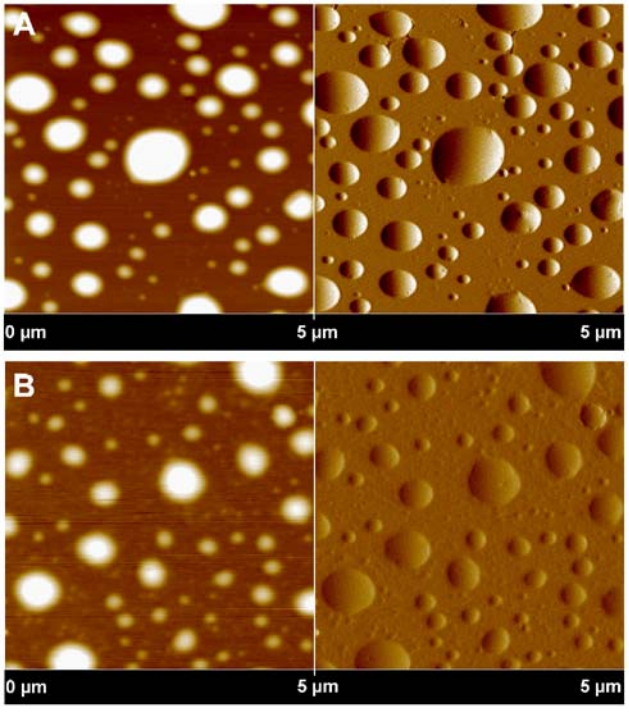

Fig. 2. Atomic force micrographs showing surface properties of polymer nanoparticles prepared from (A) PVA_{300}-g-PLGA(15), and (B) fluorescence-labelled PVA_{300}-g-PLGA(15). Each single image has an edge length of 5 µm.

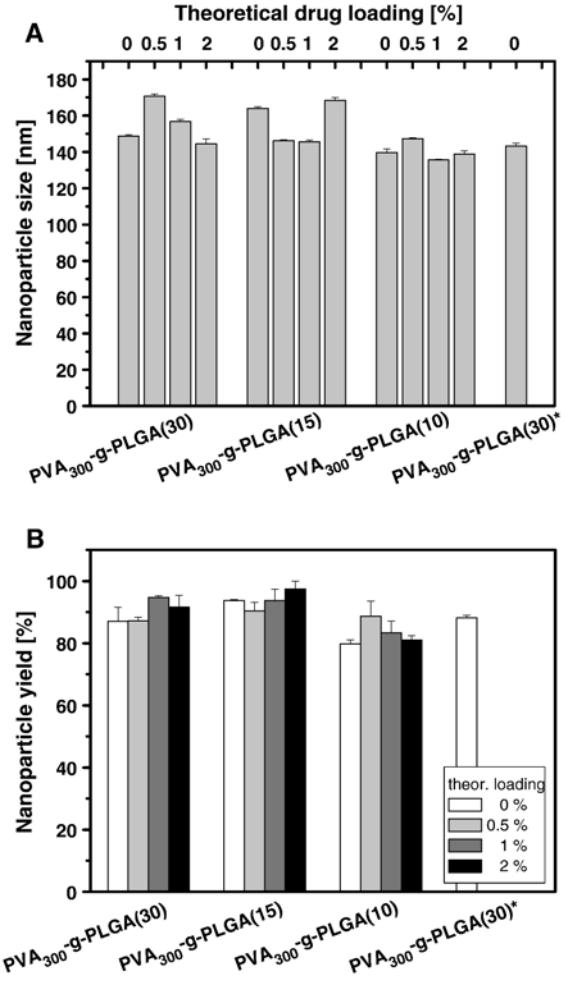

Fig. 3. (A) Size of nanoparticles (NP) prepared from three different PVA_{300}-g-PLGA comb polyesters determined by photon correlation spectroscopy. PVA_{300}-g-PLGA(30)* = NP batch for size determination after passage through a channelled balloon delivery catheter (SCIMED REMEDY™). All measurements were performed in triplicate. (B) Yield of nanoparticles prepared from three different PVA300-g-PLGA comb polyesters. It is expressed as the ratio between the polymer mass in the suspension and the theoretical amount. PVA300-g-PLGA(30)* = NP batch for yield determination after passage through a channelled balloon delivery catheter (SCIMED REMEDY ™). All measurements were performed in triplicate.

solvent. After evaporation of the organic solvent drug re-adsorbs to the nanoparticle surface.

Nevertheless, the burst release is clinically desirable to achieve initial high drug concentrations in the target tissue. After release of a loading dose, the following, and substantial sustained drug release rate is to obtain a constant drug level to prevent excessive VSMC proliferation persistently. Previous results of in vitro cell culture studies showed a paclitaxel-induced decrease in cell viability of human VSMC at a drug concentration range of 0.1 to 10 μmol/l, which is potentially favorable for local delivery. An increase in cell apoptosis was observed at higher drug levels (50 to 100 μmol/l) [12]. The intimal VSMC proliferation that follows vascular injury during angioplasty procedures reaches a maximum at 10 to 14 days and ends upon re-endothelization of the traumatized vessel segment. But due to a relatively short residence time of paclitaxel in VSMC, the application of free drug containing solutions could be less efficient to inhibit restenosis, as demonstrated for bovine VSMC [39], which underlines the need of sustained release dosage forms of antiproliferative drugs. By specific variation of PVA-g-PLGA polymer composition we were able to adjust the initial drug dose, which is released immediately after the infusion of the nanoparticle suspension into the vessel wall, and subsequently, delayed drug liberation provides a persistent effect on VSMC proliferation.

In order to obtain both a high drug release directly after locally delivery, as well as sustained Ptx release in the target tissue, we decided to use nanoparticles consisting of PVA-g-PLGA(30) to evaluate the effect of delivered nanoparticles on neointima formation in vivo.

3.3. In vitro cytotoxicity

The MTT test serves as an assay for proliferation and cell viability by measuring the mitochondrial activity of cells. Metabolically active cells are able to convert the yellow water-soluble tetrazolium salt (3-(4,5 dimethylthiazol-2-yl)-2,5-diphenyltetrazolium bromide) to a water-insoluble dark blue formazan by reductive cleavage of the tetrazolium ring. For in vitro cytotoxicity all components, which were used for nanoparticle preparation, were tested. The suspension stabilizer poloxamer 188 did not decrease the viability of RbVSMC up to concentrations of 10 mg/ml (data not shown). Pistel et al. have already demonstrated the good biocompatibility of PVA-g-PLGA polymer using the extraction method [21]. The non-toxic character of unloaded nanoparticles prepared from PVA_{300}-g-PLGA(30) and PVA_{300}-g-PLGA(15) was confirmed up to a NP concentration of approx. 370 μg/ml, as shown in (Fig. 5). By contrast paclitaxel-loaded PVA-g-PLGA nanoparticles showed a concentration dependent viability of RbVSMC. An increase of nanoparticle concentration from 3 to more than 300 μg/ml was accompanied by a reduction in cell viability of 30%. Furthermore, and this effect highlights the rationale for the encapsulation of antiproliferative drugs for local vascular delivery, at higher drug

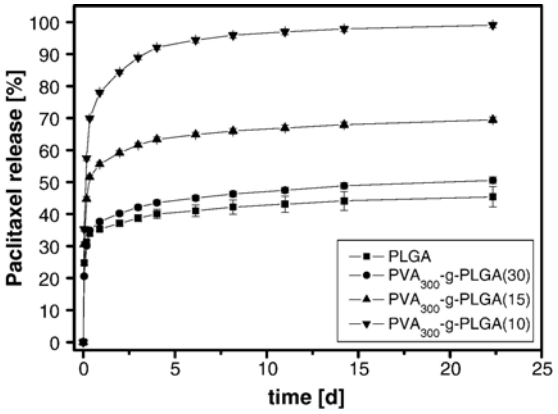

Fig. 4. Effect of the polymer composition on the in vitro paclitaxel (Ptx) release from nanoparticles loaded with 2% Ptx/14C-Ptx (mass ratio 250:1). Encapsulation efficiencies ranges from 77 to 87%. The drug released was determined by liquid scintillation counting (LSC). Each sample was measured in quadruplicate.

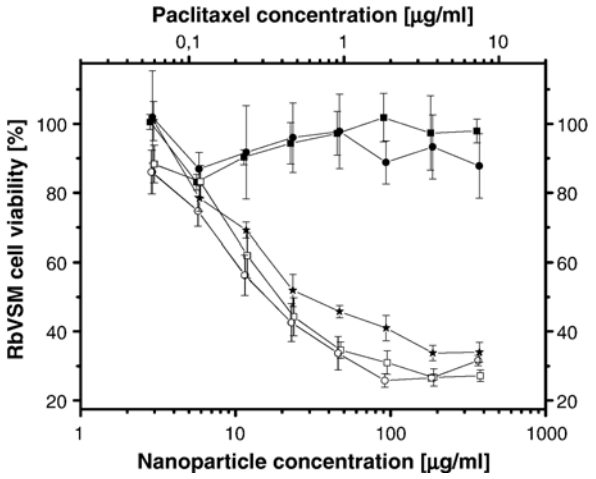

Fig. 5. Cytotoxicity of free paclitaxel (Ptx) (star symbol), blank nanoparticles (filled symbols) and Ptx-loaded nanoparticles (open symbols) (theoretical loading 2%) from PVA-g-PLGA(30) (open and filled squares) and PVA-g-PLGA(15) (open and filled circles) by means of MTT assay.

levels free paclitaxel was less toxic compared to drug-loaded nanoparticles, probably due to a higher cellular uptake of nanoparticles. Hence, nanoparticles formed a depot from which the paclitaxel is released continuously after the initial burst.

3.4. Nanoparticle uptake into RbVSMC

Confocal laser scanning microscopy of VSMC exposed to fluorescence-labeled nanoparticles loaded with 0.1% of Oregon Green labeled paclitaxel (green fluorescence) demonstrated an increasing fluorescence activity in the cells during the incubation with NP suspension for 80 min (Fig. 6). As already mentioned, the blue fluorescence of the coumarin labelled polymer in the images were changed into red color in favor of a better illustration of the co-localized nanoparticles and paclitaxel. Based on results from the in vitro cytotoxicity test, fluorescently labelled paclitaxel did not affect cell viability of VSMC negatively during NP uptake experiments. The images shown are *z*-sections through the center of the cells and confirm that the fluorescence observed is the result of nanoparticle localization inside the cells and not on the membrane surface. The co-localization of NP and paclitaxel fluorescence appeared in yellow fluorescence as a consequence of NP internalization.

Various processes, such as phagocytosis [40], receptor mediated endocytosis, or fluid phase pinocytosis [39] are hypothesized for cellular uptake of particulate drug carriers. In fact phagocytosis is generally associated with the uptake of large particles (>500 nm) and not with NP of about 100–200 nm, which was confirmed by testing the phagocytic activity of human VSMC in the presence of NP in vitro [33].

As shown in Fig. 6, the nanoparticle distribution is comparable to those reported for 6-coumarin-loaded nanoparticles [41]. Particles are arranged in vesicles, suggesting that they are probably located in the endosomal/lysosomal compartments surrounding the nucleus [39,42]. The appearance of diffuse green and red fluorescence indicates a subsequent NP escape into the cytoplasm, as hypothesized by Panyam et al. [42]. As a result of uptake inhibition at low temperatures and saturation kinetics during incubation with poly(ethylene oxide)-poly (lactide-co-glycolide) NP, Suh et al. proposed that the uptake is through adsorptive pinocytosis [39]. In contrast it was also demonstrated that in parts PLGA NP without any specific ligands were internalized nonspecifically through clathrin vesicles which are known to be involved in active receptor mediated endocytosis [42].

However, further investigations with regard to the mechanism of nanoparticle uptake and the kinetics of drug uptake and retention in the VSMC will be helpful to establish the efficiency of PVA-g-PLGA nanoparticles for the prevention of excessive proliferation of VSMC after balloon angioplasty.

3.5. Effect of locally delivered nanoparticles on neointima formation

Early pharmacological strategies to prevent post angioplasty restenosis have been focused on the systemic administration of antirestenotic drugs. Despite promising results in several animal models of restenosis [43], human trials could not fulfill the expectations.

Therefore, novel approaches for a more effective site-specific drug delivery are being directed toward local delivery

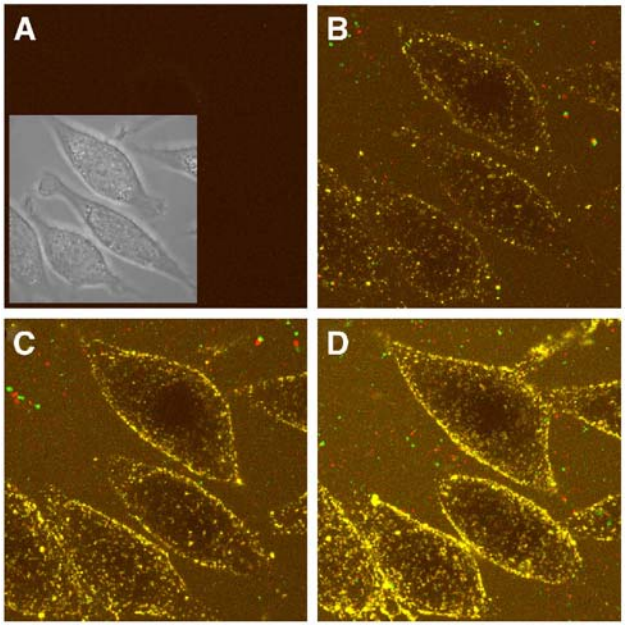

Fig. 6. CLSM images demonstrating intracellular nanoparticle distribution in RbVSMC (A) directly after incubation, (B) after 20 min, (C) after 40 min, (D) after 80 min of incubation; Oregon Green labelled paclitaxel (green), fluorescence-labelled PVA300-g-PLGA(15) (blue coumarin fluorescent label is displayed in red, see text for explanation). The insert in (A) is a differential interference contrast image showing the outline of the cells. Overlay of (A)–(D) displays co-localization of nanoparticles and paclitaxel. Each image shown is a *z*-section through the center of the cells supporting location of nanoparticles inside the cells. Nanoparticles with 0.1% theoretical loading of fluorescence-labelled paclitaxel have a diameter of 118.4 nm ± 7.3 (polydispersity index 0.1 ± 0.024). (For interpretation of the references to colour in this figure legend, the reader is referred to the web version of this article.)

systems rather than systemic administration [1]. A combination of local delivery and controlled drug release has the potential to achieve high and sustained tissue levels of the drug at the site of balloon injury, as well as to prevent adverse side effects as a consequence of a systemic administration [1,44].

To evaluate the efficiency of paclitaxel-loaded PVA-g-PLGA nanoparticles on neointima formation after balloon injury in a New Zealand white rabbit iliac artery model, we compared nanoparticle treated with control vessel segments. Other research groups have focused on a rat carotid model of vascular injury and intraluminal delivery to study the antirestenotic potential of drug-loaded nanoparticles. Amongst others they observed a particle size-dependent effect on neointima formation due to a higher uptake of the smaller tyrphostins-loaded nanoparticles [16,45]. A size-dependent nanoparticle penetration into the vessel wall was also reported by Westedt et al. While fluorescence-labelled polystyrene nanoparticles of about 100 and 200 nm were deposited in the inner regions of the vessel wall, nanoparticles larger than 500 nm accumulated primarily at the luminal surface of the aorta abdominalis in New Zealand white rabbits [46].

Based on results from Kimura et al., it can be concluded, that vascular damage and intimal thickening is associated with the degree of infusion pressure achieved by local delivery, whereas a 5 atm infusion pressure may mark the critical value, beyond which severe vascular damage occurs [47]. In the present study balloon dilatation at a pressure of 8 atm as well as the local delivery procedures at 2 atm were technically successful in all animals. All vessels were patent at completion angiography. Acute thrombosis or perforation of the target vessels was not observed in any animal. Although the local nanoparticle delivery at accelerated infusion pressures of 4 atm lead to effective nanoparticle delivery without severe vessel wall disruptions [48], the infusion pressure was reduced to 2 atm to prevent vascular damage by the relatively high suspension volume of 4 ml.

Fig. 7 shows the morphometric results of local nanoparticle application. There was a significantly smaller neointima cross sectional area in the arteries treated with nanoparticles compared to the control group. A 50% reduction in neointimal area in vessel segments treated with paclitaxel-loaded nanoparticles compared to control vessel segments was observed (local paclitaxel nanoparticle treated segments 0.80 ± 0.19 mm^2, Fig. 7A; control segments 1.58 ± 0.6 mm^2, Fig. 7B; $p < 0.05$). Although maximum concentration of placebo nanoparticles used in the in vitro VSMC model was lower than the particle concentration used for the animal experiment, we assumed that the antirestenotic effect was caused by paclitaxel, which was released from the nanoparticles. Based on previously reported data, a PVA-g-PLGA concentration of up to 100 mg/ml led to a reduction of cell viability of ca. 20% in a L929 fibroblasts cell culture model, and was very similar to linear PLGAs, which underlines the non-toxic character of branched polyesters [21].

The implications of this experimental study on the clinical situation in humans are uncertain and extrapolation of these data requires caution. Although dose conversion factors for interspecies extrapolation has already been identified [49], the effective doses in animals cannot be safely extrapolated to humans due to significant differences between animal and human pharmacokinetics and metabolism [43]. Furthermore, as in most experimental studies the major limitation of this study is related to the animal model being used. Although the hypercholesterolemic and/or denudated rabbit iliac artery model produces considerable smooth muscle cell proliferation and intimal hyperplasia, it is well recognized that this response may be insufficient to create obstructive atherosclerotic disease. The situation in atherosclerotic or restenotic lesions will differ vastly because of (i) worse catheter adherence to the irregular vessel wall, (ii) diffusion barriers due to calcification and scar tissue. Therefore, parts of the suspension may escape between the vessel wall and the delivery balloon, and reach the systemic circulation. Moreover, nanoparticles can leak from the vessel wall through the infusion channels back into the vessel lumen [48]. For this reason, a conclusive statement with respect to the delivery efficiency was not possible. Therefore, it has to be taken into account that additionally to its antiproliferative impact, paclitaxel causes adverse hematopoietic effects in a dose-dependent manner when reaching the blood circulation [43,44].

Nevertheless, the drug delivery concept constitutes a combined mechanical and pharmacologic approach that appears as a promising preventive strategy against restenosis. Apart from catheter-based local drug delivery there are other promising

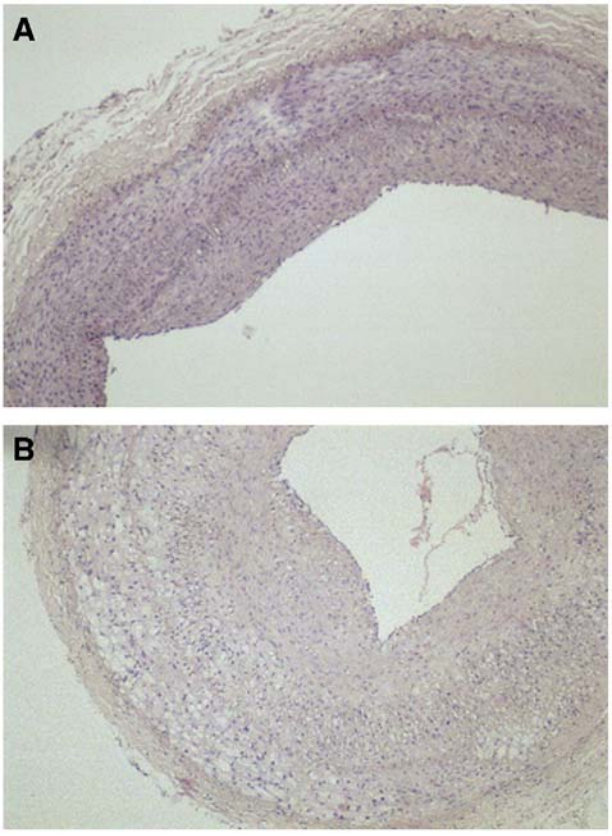

Fig. 7. Photomicrographs of common iliac arteries (hematoxyline-eosin staining; microscopic magnification 40×) of cholesterol fed rabbits. Neointimal area (NA) is markedly reduced in vessel segments treated with paclitaxel-loaded nanoparticles (A) compared to control segments treated with saline under similar conditions (B).

approaches to prevent restenosis after balloon angioplasty, especially intravascular brachytherapy [50] as well as drug coated and drug eluting stents [51]. However, especially coated stents have potential disadvantages. Most of the current stent designs cover only 5% to 12% of the arterial surface, limiting the amount of surface area in contact with the drug. In addition, use of a prosthetic, permanent stent implant is undesirable for the purpose of a short-term drug delivery. In view of the rapidly involving field of new therapeutic approaches, local delivery devices seem to be of great interest especially in peripheral artery occlusive disease and deserve further investigation in clinical trials.

4. Conclusions

This study describes the formulation of biodegradable nanoparticles (<180 nm) using solvent displacement technique for catheter-based local intraluminal drug delivery. PVA-g-PLGA comb polyesters are suitable biodegradable polymers for the nanoencapsulation of paclitaxel. By varying the composition of PVA-g-PLGA polymers the release kinetics can be adapted to the clinical requirements of drug delivery for prevention of restenosis. We have further demonstrated that unloaded PVA-g-PLGA nanoparticles are non-toxic to RbVSMC and capable of sustained intracellular delivery of paclitaxel. Paclitaxel-loaded nanoparticles decrease the cell viability of RbVSMC in vitro more effective than the free drug. Confocal laser scanning microscopy confirmed the uptake of paclitaxel-loaded nanoparticles. It has to be noted that the relevance of the present results to human clinical circumstance is uncertain. Furthermore, long-term effects of studied nanoparticle formulations are not known. Despite those study limitations the local administration of these particles to common iliac arteries of New Zealand white rabbits was associated with a significant decrease in neointimal formation. These findings support the rationale for the design of colloidal drug delivery systems based on biodegradable nanoparticles from poly(vinyl alcohol)-g-lactide-co-glycolide), which offer attractive features for the prevention of restenosis after angioplasty.

The composition of branched polyesters can be varied to meet the needs of almost any antirestenotic compound like lipophilic drugs as paclitaxel, as well as hydrophilic, macromolecular drugs, such as peptides, proteins [52], or DNA [53], which have the potential for the treatment of restenosis. The modification of PLGA side chain length and PVA backbone composition lead to a more versatile polymer platform compared to commonly used PLA and PLGA [54].

Acknowledgements

We would like to thank Nicole Bamberger, Beate Kleb and Michael Hellwig for their valuable technical assistance. Further on, we gratefully acknowledge financial support of the project Ki 592/5-1 by Deutsche Forschungsgemeinschaft (DFG), Sam Yang Corporation Seoul, Korea for providing Genexol™, and Boston Scientific Natick, MA for providing SCIMED REMEDY™ channelled balloon catheters.

References

[1] M. Chorny, I. Fishbein, G. Golomb, Drug delivery systems for treatment of restenosis, Crit. Rev. Ther. Drug Carr. Syst. 17 (3) (2000) 249–284.
[2] J.A. Dormandy, R.B. Rutherford, Management of peripheral arterial disease (PAD). TASC Working Group. TransAtlantic Inter-Society Concensus (TASC), J. Vasc. Surg. 31 (1 Pt 2) (2000) S1–S296.
[3] T. Jaemsen, H. Manninen, H. Tulla, P. Matsi, The final outcome of primary infrainguinal percutaneous transluminal angioplasty in 100 consecutive patients with chronic critical limb ischemia, J. Vasc. Interv. Radiol. 13 (5) (2002) 455–463.
[4] J.J. Popma, R.M. Califf, E.J. Topol, Clinical trials of restenosis after coronary angioplasty, Circulation 84 (3) (1991) 1426–1436.
[5] C. Bauters, J.M. Isner, The biology of restenosis, Prog. Cardiovasc. Dis. 40 (2) (1997) 107–116.
[6] B. Bhargava, G. Karthikeyan, A.S. Abizaid, R. Mehran, New approaches to preventing restenosis, Br. Med. J. 327 (7409) (2003) 274–279.
[7] D.W. Muller, E.J. Topol, G.D. Abrams, K.P. Gallagher, S.G. Ellis, Intramural methotrexate therapy for the prevention of neointimal thickening after balloon angioplasty, J. Am. Coll. Cardiol. 20 (2) (1992) 460–466.
[8] J.F. Mitchel, D.B. Fram, D.F. Palme, R. Foster, J.A. Hirst, M.A. Azrin, L.M. Bow, A.M. Eldin, D.D. Waters, R.G. McKay, Enhanced intracoronary thrombolysis with urokinase using a novel, local drug delivery system. In vitro, in vivo, and clinical studies, Circulation 91 (3) (1995) 785–793.
[9] J. Rome, V. Shayani, M. Flugelman, K. Newman, A. Farb, R. Virmani, D. Dichek, Anatomic barriers influence the distribution of in vivo gene transfer into the arterial wall. Modeling with microscopic tracer particles and verification with a recombinant adenoviral vector, Arterioscler. Thromb. 14 (1) (1994) 148–161.
[10] I. Gradus-Pizlo, R.L. Wilensky, K.L. March, N. Fineberg, M. Michaels, G.E. Sandusky, D.R. Hathaway, Local delivery of biodegradable microparticles containing colchicine or a colchicine analogue: effects on restenosis and implications for catheter-based drug delivery, J. Am. Coll. Cardiol. 26 (6) (1995) 1549–1557.
[11] T.K. Nasser, R.L. Wilensky, K. Mehdi, K.L. March, Microparticle deposition in periarterial microvasculature and intramural dissections after porous balloon delivery into atherosclerotic vessels: quantitation and localization by confocal scanning laser microscopy, Am. Heart J. 131 (5) (1996) 892–898.
[12] D.I. Axel, W. Kunert, C. Goggelmann, M. Oberhoff, C. Herdeg, A. Kuttner, D.H. Wild, B.R. Brehm, R. Riessen, G. Koveker, K.R. Karsch, Paclitaxel inhibits arterial smooth muscle cell proliferation and migration in vitro and in vivo using local drug delivery, Circulation 96 (2) (1997) 636–645.
[13] C. Herdeg, M. Oberhoff, A. Baumbach, A. Blattner, D.I. Axel, S. Schroder, H. Heinle, K.R. Karsch, Local paclitaxel delivery for the prevention of restenosis: biological effects and efficacy in vivo, J. Am. Coll. Cardiol. 35 (7) (2000) 1969–1976.
[14] E.K. Rowinsky, R.C. Donehower, Paclitaxel (Taxol), N. Engl. J. Med. 332 (15) (1995) 1004–1014.
[15] H. Fessi, J.P. Devissaguet, F. Puisieux, C. Thies, Process of the preparation of dispersable colloidal systems of a substance in the form of nanoparticles formation of colloidal nanoparticles, 5, 118,528, 1992.
[16] I. Fishbein, M. Chorny, L. Rabinovich, S. Banai, I. Gati, G. Golomb, Nanoparticulate delivery system of a tyrphostin for the treatment of restenosis, J. Control. Release 65 (1–2) (2000) 221–229.
[17] C. Song, V. Labhasetwar, X. Cui, T. Underwood, R.J. Levy, Arterial uptake of biodegradable nanoparticles for intravascular local drug delivery: results with an acute dog model, J. Control. Release 54 (2) (1998) 201–211.
[18] L. Mu, S.S. Feng, A novel controlled release formulation for the anticancer drug paclitaxel (Taxol): PLGA nanoparticles containing vitamin E TPGS, J. Control. Release 86 (1) (2003) 33–48.
[19] K.S. Soppimath, T.M. Aminabhavi, A.R. Kulkarni, W.E. Rudzinski, Biodegradable polymeric nanoparticles as drug delivery devices, J. Control. Release 70 (1–2) (2001) 1–20.
[20] A. Breitenbach, T. Kissel, Biodegradable comb polyesters: Part 1—synthesis, characterisation and structural analysis of PLA and PLGA

grafted onto water-soluble PVA as backbone, Polymers 39 (14) (1998) 3261–3271.
[21] K.F. Pistel, A. Breitenbach, R. Zange, T. Kissel, Brush-like biodegradable polyesters, Part III, protein release from microspheres of poly(vinyl alcohol)-graft-poly(D,L-lactic-co-glycolic acid), J. Control. Release 73 (1) (2001) 7–20.
[22] A. Breitenbach, K.F. Pistel, T. Kissel, Biodegradable comb polyesters Part II. Erosion and release properties of PVA-g-PLG, Polymers 41 (2000) 4781–4792.
[23] T. Jung, A. Breitenbach, T. Kissel, Sulfobutylated poly(vinyl alcohol)-graft-poly(lactide-co-glycolide)s facilitate the preparation of small negatively charged biodegradable nanospheres, J. Control. Release 67 (2–3) (2000) 157–169.
[24] S.M. Ropiak, Multiple Hole Drug Delivery Balloon, US 5,860,954, 1999.
[25] V. Oberle, U. Bakowsky, I.S. Zuhorn, D. Hoekstra, Lipoplex formation under equilibrium conditions reveals a three-step mechanism, Biophys. J. 79 (3) (2000) 1447–1454.
[26] D.I. Axel, B.R. Brehm, K. Wolburg-Buchholz, E.L. Betz, G. Koveker, K.R. Karsch, Induction of cell-rich and lipid-rich plaques in a transfilter coculture system with human vascular cells, J. Vasc. Res. 33 (4) (1996) 327–339.
[27] D. Quintanar-Guerrero, E. Allémann, E. Doelker, H. Fessi, A mechanistic study of the formation of polymer nanoparticles by the emulsification–diffusion technique, Colloid Polym. Sci. 275 (7) (1997) 640–647.
[28] S. Feng, G. Huang, Effects of emulsifiers on the controlled release of Paclitaxel (Taxol) from nanospheres of biodegradable polymers, J. Control. Release 71 (1) (2001) 53–69.
[29] C. Fonseca, S. Simoes, R. Gaspar, Paclitaxel-loaded PLGA nanoparticles: preparation, physicochemical characterization and in vitro anti-tumoral activity, J. Control. Release 83 (2) (2002) 273–286.
[30] X. Jingwei, W. Chi-Hwa, Self-assembled biodegradable nanoparticles developed by direct dialysis for the delivery of paclitaxel, Pharm. Res. 22 (12) (2005) 2079–2090.
[31] U. Westedt, M. Wittmar, M. Hellwig, P. Hanefeld, A. Greiner, A.K. Schaper, T. Kissel, Paclitaxel releasing films consisting of poly(vinyl alcohol)-graft-poly(lactide-co-glycolide) and their potential as biodegradable stent coatings, J. Control. Release 111 (1–2) (2006) 235–246.
[32] J.S. Chawla, M.M. Amiji, Cellular uptake and concentrations of tamoxifen upon administration in poly(epsilon–caprolactone) nanoparticles, AAPS PharmSci 5 (1) (2003) E3.
[33] J. Panyam, V. Labhasetwar, Dynamics of endocytosis and exocytosis of poly(D,L-lactide-co-glycolide) nanoparticles in vascular smooth muscle cells, Pharm. Res. 20 (2) (2003) 212–220.
[34] M. Chorny, I. Fishbein, H.D. Danenberg, G. Golomb, Study of the drug release mechanism from tyrphostin AG-1295-loaded nanospheres by in situ and external sink methods, J. Control. Release 83 (3) (2002) 401–414.
[35] S.S. Feng, L. Mu, K.Y. Win, G. Huang, Nanoparticles of biodegradable polymers for clinical administration of paclitaxel, Curr. Med. Chem. 11 (4) (2004) 413–424.
[36] R.H. Muller, K. Maeder, S. Gohla, Solid lipid nanoparticles (SLN) for controlled drug delivery — a review of the state of the art, Eur. J. Pharm Biopharm. 50 (1) (2000) 161–177.
[37] J.S. Chawla, M.M. Amiji, Biodegradable poly(epsilon–caprolactone) nanoparticles for tumor-targeted delivery of tamoxifen, Int. J. Pharm. 249 (1–2) (2002) 127–138.
[38] I. Brigger, P. Chaminade, V. Marsaud, M. Appel, M. Besnard, R. Gurny, M. Renoir, P. Couvreur, Tamoxifen encapsulation within polyethylene glycol-coated nanospheres. A new antiestrogen formulation, Int. J. Pharm. 214 (1–2) (2001) 37–42.
[39] H. Suh, B. Jeong, R. Rathi, S.W. Kim, Regulation of smooth muscle cell proliferation using paclitaxel-loaded poly(ethylene oxide)-poly(lactide/glycolide) nanospheres, J. Biomed. Mater. Res. 42 (2) (1998) 331–338.
[40] K.A. Foster, M. Yazdanian, K.L. Audus, Microparticulate uptake mechanisms of in-vitro cell culture models of the respiratory epithelium, J. Pharm. Pharmacol. 53 (1) (2001) 57–66.
[41] J. Panyam, S.K. Sahoo, S. Prabha, T. Bargar, V. Labhasetwar, Fluorescence and electron microscopy probes for cellular and tissue uptake of poly(D,L-lactide-co-glycolide) nanoparticles, Int. J. Pharm. 262 (1–2) (2003) 1–11.
[42] J. Panyam, W.Z. Zhou, S. Prabha, S.K. Sahoo, V. Labhasetwar, Rapid endo-lysosomal escape of poly(D,L-lactide-co-glycolide) nanoparticles: implications for drug and gene delivery, FASEB J. 16 (10) (2002) 1217–1226.
[43] D.W. Kim, J.S. Kwon, Y.G. Kim, M.S. Kim, G.S. Lee, T.J. Youn, M.C. Cho, Novel oral formulation of paclitaxel inhibits neointimal hyperplasia in a rat carotid artery injury model, Circulation 109 (12) (2004) 1558–1563.
[44] S. Yasuda, T. Noguchi, M. Gohda, T. Arai, N. Tsutsui, Y. Nakayama, T. Matsuda, H. Nonogi, Local delivery of low-dose docetaxel, a novel microtubule polymerizing agent, reduces neointimal hyperplasia in a balloon-injured rabbit iliac artery model, Cardiovasc. Res. 53 (2) (2002) 481–486.
[45] I. Fishbein, M. Chorny, S. Banai, A. Levitzki, H.D. Danenberg, J. Gao, X. Chen, E. Moerman, I. Gati, V. Goldwasser, G. Golomb, Formulation and delivery mode affect disposition and activity of tyrphostin-loaded nanoparticles in the rat carotid model, Arterioscler. Thromb. Vasc. Biol. 21 (9) (2001) 1434–1439.
[46] U. Westedt, L. Barbu-Tudoran, A.K. Schaper, M. Kalinowski, H. Alfke, T. Kissel, Deposition of nanoparticles in the arterial vessel by porous balloon catheters: localisation by confocal laser scanning microscopy and transmission electron microscopy, AAPS PharmSci 4 (4) (2002) (article 41).
[47] T. Kimura, K. Miyauchi, S. Yamagami, H. Daida, H. Yamaguchi, Local delivery infusion pressure is a key determinant of vascular damage and intimal thickening, Jpn. Circ. J. 62 (4) (1998) 299–304.
[48] U. Westedt, L. Barbu-Tudoran, A.K. Schaper, M. Kalinowski, H. Alfke, T. Kissel, Effects of different application parameters on penetration characteristics and arterial vessel wall integrity after local nanoparticle delivery using a porous balloon catheter, Eur. J. Pharm. Biopharm. 58 (1) (2004) 161–168.
[49] E.J. Freireich, E.A. Gehan, D.P. Rall, L.H. Schmidt, H.E. Skipper, Quantitative comparison of toxicity of anticancer agents in mouse, rat, hamster, dog, monkey, and man, Cancer Chemother. Rep. 50 (4) (1966) 219–244.
[50] P.S. Teirstein, R.E. Kuntz, New frontiers in interventional cardiology: intravascular radiation to prevent restenosis, Circulation 104 (21) (2001) 2620–2626.
[51] J.E. Sousa, M.A. Costa, A. Abizaid, A.G. Sousa, F. Feres, L.A. Mattos, M. Centemero, G. Maldonado, A.S. Abizaid, I. Pinto, R. Falotico, J. Jaeger, J.J. Popma, P.W. Serruys, Sirolimus-eluting stent for the treatment of in-stent restenosis: a quantitative coronary angiography and three-dimensional intravascular ultrasound study, Circulation 107 (1) (2003) 24–27.
[52] C.P. Cruz, J. Eidt, J. Drouilhet, A.T. Brown, Y. Wang, C.S. Barnes, M.M. Moursi, Saratin, an inhibitor of von Willebrand factor-dependent platelet adhesion, decreases platelet aggregation and intimal hyperplasia in a rat carotid endarterectomy model, J. Vasc. Surg. 34 (4) (2001) 724–729.
[53] C.G. Oster, M. Wittmar, F. Unger, L. Barbu-Tudoran, A.K. Schaper, T. Kissel, Design of amine-modified graft polyesters for effective gene delivery using DNA-loaded nanoparticles, Pharm. Res. 21 (6) (2004) 927–931.
[54] L.A. Dailey, M. Wittmar, T. Kissel, The role of branched polyesters and their modifications in the development of modern drug delivery vehicles, J. Control. Release 101 (1–3) (2005) 137–149.